JOURNAL OF VIROLOGY, Apr. 1997, p. 3129–3137 Vol. 71, No. 4
0022-538X/97/$04.00+0
Copyright © 1997, American Society for Microbiology

A Role for Naturally Occurring Variation of the Murine Coronavirus Spike Protein in Stabilizing Association with the Cellular Receptor

THOMAS M. GALLAGHER*

Department of Microbiology and Immunology, Loyola University Medical Center, Maywood, Illinois 60153

Received 29 August 1996/Accepted 18 December 1996

Murine hepatitis virus (MHV), a coronavirus, initiates infection by binding to its cellular receptor (MHVR) via spike (S) proteins projecting from the virion membrane. The structures of these S proteins vary considerably among MHV strains, and this variation is generally considered to be important in determining the strain-specific pathologies of MHV infection, perhaps by affecting the interaction between MHV and the MHVR. To address the relationships between S variation and receptor binding, assays capable of measuring interactions between MHV and MHVR were developed. The assays made use of a novel soluble form of the MHVR, sMHVR-Ig, which comprised the virus-binding immunoglobulin-like domain of MHVR fused to the Fc portion of human immunoglobulin G1. sMHVR-Ig was stably expressed as a disulfide-linked dimer in human 293 EBNA cells and was immobilized to Sepharose-protein G via the Fc domain. The resulting Sepharose beads were used to adsorb radiolabelled MHV particles. At 4°C, the beads specifically adsorbed two prototype MHV strains, MHV JHM (strain 4) and a tissue culture-adapted mutant of MHV JHM, the JHMX strain. A shift to 37°C resulted in elution of JHM but not JHMX. This in vitro observation of JHM (but not JHMX) elution from its receptor at 37°C was paralleled by a corresponding 37°C elution of receptor-associated JHM (but not JHMX) from tissue culture cells. The basis for this difference in maintenance of receptor association was correlated with a large deletion mutation present within the JHMX S protein, as sMHVR-Ig exhibited relatively thermostable binding to vaccinia virus-expressed S proteins containing the deletion. These results indicate that naturally occurring mutations in the coronavirus S protein affect the stability of the initial interaction with the host cell and thus contribute to the likelihood of successful infection by incoming virions. These changes in virus entry features may result in coronaviruses with novel pathogenic properties.

As the first step in the infection of the host cell, the interaction of virions with plasma membrane receptors plays a key role in determining the outcome of infection. To deliver the genome, viral and cellular ligands must bind and then virions must undergo a series of uncoating events in the appropriate cellular location. The ligands involved in the initiation of infection by animal coronaviruses are known (34), thereby establishing these viruses as models capable of contributing to our understanding of these early infection events.

Murine hepatitis virus (MHV) is a coronavirus; virions contain a large (27- to 32-kb) positive-strand RNA genome enclosed within a membrane envelope. These viruses are assembled in the host cell when progeny RNA genomes associate closely with nucleocapsid proteins and then bud into the lumenal cavities of intracellular membrane compartments (38, 61). Envelopment of the ribonucleoprotein complex involves the participation of the following three or four virus-encoded membrane proteins: spike (S), membrane, small membrane, and (in some MHV strains) hemagglutinin (53, 54). Assembled virions are then released from the host cell after transport through the exocytic pathway. The subsequent delivery of RNA genomes from assembled virions to neighboring host cells is dependent primarily on the functions of the S protein. S proteins bind to the MHV receptor (MHVR) (13, 27) and induce the fusion of virion and cell membranes (62), thereby permitting exposure of the infectious ribonucleoprotein complex to the host cytosol.

Biochemical investigations of MHV S proteins have shown that they are large (180-kDa) type I integral membrane glycoproteins that exist as homo-oligomeric, 20-nm projections on the virion surface (15, 16). For some MHV strains, the S protein monomers that make up these projections are composed of two polypeptide chains. This is because S monomers are subjected to cleavage by a host cell protease during intracellular transport (25, 56), thereby generating a peripheral N-terminal S1 fragment and membrane-embedded C-terminal S2 fragment. The S1 fragment binds directly to the MHVR (58, 60), and the noncovalent interaction between S1 and S2 (8, 57) ensures that virions are kept near the cell surface after inoculation.

RNA sequences encoding the S1 fragment are subject to mutation, the most striking of which results in the deletion of about 450 nucleotides near the center of the S1 gene (3, 9, 48, 64). These deletion mutations are remarkably large for an RNA virus, eliminating about 20% of S1 amino acid residues. Once formed, these S1 deletion mutants appear to be selectively amplified over that of the parent virus in tissue culture (28, 49). Emerging S1 deletion mutants are also relevant to coronavirus infections in animals, as evidenced by studies of pigs infected with the highly pathogenic transmissible gastroenteritis virus. Natural deletion mutations within the S1 gene of transmissible gastroenteritis virus is tightly correlated with the generation of an attenuated pneumotropic variant that causes respiratory disease (40).

The mechanisms by which S1 deletions provide selective growth advantages to coronaviruses remain unclear. Relative

* Mailing address: Department of Microbiology and Immunology, Loyola University Medical Center, 2160 S. First Ave., Maywood, IL 60153. Phone: (708) 216-4850. Fax: (708) 216-9574. E-mail: tgallag@luc.edu.

to the parent viruses, these mutants lack both antibody epitopes (14, 28, 40, 59) and T-cell epitopes (7), thus suggesting that S1 deletion can provide a means for escape from immunologic surveillance. However, the in vivo growth kinetics of deletion mutants differs from that of the parent virus even when measured within 1 day of infection (23), before the onset of adaptive immune responses. Additionally, these mutants exhibit significant growth advantages in tissue culture (28, 49), thereby pointing to the involvement of nonimmune factors during the selective process. In this regard, one might hypothesize that S1 deletion mutations increase the likelihood of a productive entry process, perhaps at the level of virus-receptor interaction.

Detailed studies of the binding between MHV particles and the cellular receptor can now be addressed because of numerous fundamental advances in coronavirology. The MHVR has been identified (65, 66), cloned, sequenced, and found to be identical to murine biliary glycoprotein (18). Through analysis of recombinant forms of the MHVR, the domain necessary for virus binding was identified (20). This domain is structurally homologous to an immunoglobulin (Ig) fold (5), thus suggesting that the Fab domains of an antibody could be replaced by virus-binding domains to generate a chimeric MHVR-Ig protein. Such a soluble recombinant MHVR was produced and used to study the interactions between the receptor and MHV particles.

MATERIALS AND METHODS

Cells and viruses. Monolayer cultures of murine 17 cl 1 fibroblasts (55) were grown in Dulbecco's modified Eagle medium (DMEM) supplemented with 5% tryptose phosphate broth (Difco) and 5% heat-inactivated fetal calf serum (ΔFCS; Gibco). 293 EBNA (InVitroGen, Inc.), HeLa tTA (32), and HeLa-MHVR (30) cells were grown in DMEM containing 10% ΔFCS.

Murine coronaviruses were grown in 17 cl 1 cell cultures. To prepare radiolabelled virions, infected cells were incubated with labelling medium (methionine- and cysteine-free DMEM containing 1% dialyzed ΔFCS and 50 μCi of ^{35}S translabel [ICN, Inc.] per ml) from 12 to 14 h postinfection. Virions secreted into supernatant fluids during this period were isolated by equilibrium sedimentation in sucrose gradients as described previously (30). Gradient fractions were stored at −80°C.

Synthesis of recombinant receptor glycoprotein. cDNA encoding the amino-terminal domain (NTD) of the prototype MHVR (18) was amplified by PCR (36) with a forward primer containing a *Not*I site (5′GCGGCCGCAGCC*ATG* GAGCTGGCCTC3′; *Not*I site underlined and MHVR initiation codon in italics) and a reverse primer containing a *Cla*I site and a 5′ splice donor site (5′ATCGATAT*ACTTACCTG*TGGGGTGTACATGAAATC3′; *Cla*I site underlined and splice donor site in italics). The resulting 276-bp product was ligated into pGEMT (Promega, Inc.), cloned, and then amplified by transformation into *Escherichia coli* DH5α (50). The *Not*I-*Cla*I insert was excised and ligated in a three-fragment reaction with a 1.6-kbp *Cla*I-*Bam*HI fragment of genomic fetal liver DNA containing exons for the hinge, C_H2, and C_H3 of human IgG1 (22) and with the 10.4-kbp *Not*I-*Bam*HI-linearized pCEP4 vector (InVitroGen, Inc.). The final plasmid (pCEP4:sMHVR-Ig) was cloned and amplified in *E. coli* DH5α.

pCEP4:sMHVR-Ig clones (1 μg) were transfected into 293 EBNA cells (10^6 cells in 10 cm^2) by lipofection (24), and stable transfectants were selected by growth in DMEM–10% ΔFCS containing 100 μg of G418 (Gibco) per ml and 200 μg of hygromycin B (Sigma) per ml. Visible hygromycin-resistant clones emerged by 6 days posttransfection.

Media were removed from confluent monolayers of stably transfected 293 EBNA cells, poured through 0.2-μm-pore-size nitrocellulose filters, and stored at −20°C. To detect sMHVR-Ig, media proteins were electrophoresed on discontinuous sodium dodecyl sulfate (SDS)-polyacrylamide gels, transferred to nitrocellulose, and incubated overnight in phosphate-buffered saline (PBS)–2% bovine serum albumin–0.1% Tween 20 containing a 1:1,000 dilution of alkaline phosphatase (ALP)-conjugated goat antibody directed against human IgG (Cappell, Inc.). Nitrocellulose sheets were rinsed with PBS and then with 0.9% NaCl, and BCIP (5-bromo-4-chloro-3-indolylphosphate toluidinium)-NBT (nitroblue tetrazolium) reagent (Pierce Co.) was added to identify the bound ALP-antibody conjugates.

Coronavirion-receptor binding assays. (i) In vitro binding. Beads of Sepharose-protein G (Pharmacia) were incubated with gentle agitation at 0.1% (vol/vol) with DMEM–10% ΔFCS containing serial dilutions of sMHVR-Ig medium for 2 h at 22°C. These incubation conditions resulted in quantitative adsorption of sMHVR-Ig to the beads. Sepharose beads were then pelleted by centrifugation (2,000 × *g* for 5 min), resuspended in PBS to 0.1% (vol/vol), washed three times with PBS via cycles of centrifugation and resuspension, and mixed with DMEM–1% ΔFCS to 1% (vol/vol).

In typical binding assays, 0.01 to 0.1 ml of purified ^{35}S-labelled virions {in 25 mM sodium-PIPES [piperazine-*N*,*N*′-bis(2-ethanesulfonic acid)] [pH 6.5], 100 mM NaCl, 0.01% bovine serum albumin, 40% [wt/wt] sucrose} was mixed with 0.1 ml of 1% (vol/vol) sMHVR-Ig beads and the final volume was adjusted to 1 ml by the addition of DMEM–1% ΔFCS. Adsorption was allowed to continue for 18 to 36 h at 4°C with gentle agitation. Beads were pelleted, supernatants were removed and saved, and bead-containing pellets were resuspended in 1 ml of 1% SDS. The radioactivities associated with 0.2-ml aliquots of supernatant and pellet fractions were counted by scintillation spectrometry.

(ii) In vivo (tissue culture cell) binding. HeLa-MHVR cells (clone 3) (30) were grown to confluence in monolayer cultures, and then media were removed and replaced with ice-cold DMEM–0.1% ΔFCS containing purified ^{35}S-labelled virions. After overnight incubation at 4°C, unadsorbed virions were removed and cells were rinsed five times with ice-cold DMEM–0.1% ΔFCS and then lysed with DMEM–0.1% ΔFCS containing 1% Nonidet P-40 (NP-40). Cell lysate- and supernatant-associated radioactivities were quantitated.

Vaccinia virus-mediated S expression. To obtain a vaccinia virus recombinant encoding an S protein lacking S1 codons 446 to 598 (nucleotides 1336 to 1794; numbering according to that of Parker et al. [48]), RNA was isolated from JHMX-infected 17 cl 1 cells at 12 h postinfection by the RNAzol B method (12) and then cDNA was prepared with random hexanucleotide primers and avian myeloblastosis virus reverse transcriptase (Promega). The resulting cDNA preparation was used as the template in PCR (37) with primers S1-1 and S1-2 (1). The purified 373-bp PCR DNA was digested with *Bsp*EI and *Msc*I (New England Biolabs), resulting in a 201-bp restriction fragment which was used to replace the corresponding 660-bp *Bsp*EI-*Msc*I fragment excised from pTM1-S_4 (30, 45). Recombinant plasmid pTM1-$S_{\Delta S1}$ was cloned and amplified in *E. coli* DH5α and sequenced (51) to confirm the absence of S1 nucleotides. pTM1-S constructs were recombined into the thymidine kinase (TK) gene of vaccinia virus (strain WR), and TK$^-$ recombinant viruses were selected by standard methodologies (42). TK$^-$ virus stocks were then screened for the synthesis of functional S proteins by inoculation onto HeLa-MHVR cells in conjunction with vTF7.3 (26). Those stocks able to induce overt syncytia were saved at −80°C.

Coronavirus S protein-receptor binding assay. At 12 h after infection of HeLa tTA cell monolayers (10^6 cells in 10 cm^2) with vTF7.3 and the respective vTM1-S recombinants, cells were chilled on ice and overlaid with ice-cold sMHVR-Ig (10 μg per well in 1 ml of DMEM–10% ΔFCS). After 2 h at 4°C, unbound sMHVR-Ig was removed and replaced with ice-cold DMEM–0.1% ΔFCS containing 5 μg of brefeldin A per ml (1 ml per well). Brefeldin A was present to arrest further transport of S proteins to the cell surface. At various times after a shift to 37°C, supernatants were removed and cells were dissolved in DMEM–0.1% ΔFCS containing 0.5% NP-40 (1 ml per well). sMHVR-Ig in cell and supernatant fractions was precipitated with Sepharose-protein G and identified by Western immunoblotting.

RESULTS

Synthesis and analysis of the recombinant sMHVR-Ig. A recombinant MHVR that could be tethered at various densities to a solid phase would permit detailed investigation of the virion-receptor interaction. An MHVR with these capabilities was produced by covalently linking the NTD (virus-binding domain) of the MHVR ($MHVR_{NTD}$) to the Fc domain of an antibody. To this end, a PCR cDNA clone of $MHVR_{NTD}$ (20) was ligated to a genomic fragment of human fetal liver DNA harboring exons for the hinge, C_H2, and C_H3 of IgG1 (22). The resulting product was inserted into the episomal Epstein-Barr virus-based expression vector pCEP4 and then transfected by lipofection into 293 EBNA cells. Cell lines maintaining pCEP4:sMHVR-Ig episomes were selected with antibiotic medium, as described in Materials and Methods.

Stably transfected cells were expected to secrete a polypeptide with the characteristics depicted in Fig. 1A. The predicted molecule, termed sMHVR-Ig, is a 90-kDa disulfide-linked glycoprotein dimer, with each 45-kDa monomer consisting of the $MHVR_{NTD}$, C_H2, and C_H3 Ig domains. A dimeric receptor was actually desired because cross-linking studies have suggested that the authentic MHVR is a dimer (21). To identify the anticipated product, culture supernatants were subjected to immunoblot analysis using detection reagents specific for the human IgG1 Fc domain. Immunoblot profiles (Fig. 1B) verified the existence of a ca. 45-kDa monomer and a ca.

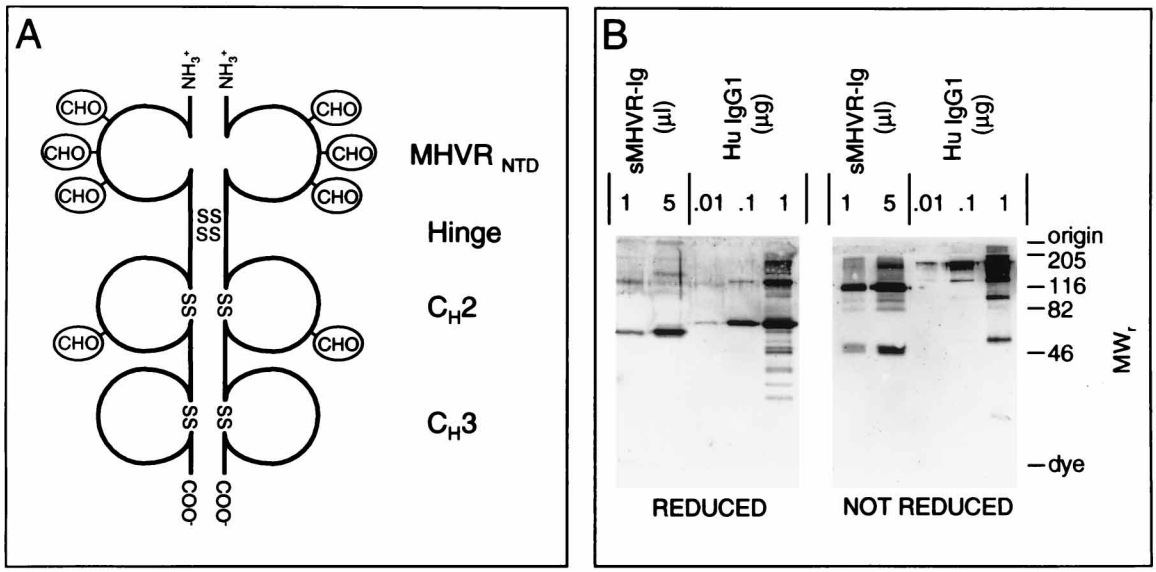

FIG. 1. Schematic depiction (A) and Western immunoblot analysis (B) of sMHVR-Ig. (A) sMHVR-Ig glycoprotein is pictured as a disulfide-linked dimer, with each monomer consisting of three ca. 110-residue Ig domains. C_H2 and C_H3 of human IgG1 comprise the two carboxy-terminal domains. The NTD consists of residues 35 to 141 of the prototype MHVR (also known as biliary glycoprotein isoform 1[a]). These residues function in virus binding. Intermolecular disulfides (SS) are presumed to be within the 15-residue hinge of human IgG1, which separates the $MHVR_{NTD}$ from the C_H2 and C_H3 domains. CHO, N-linked carbohydrates. (B) The indicated volumes of conditioned media from stable 293 EBNA–sMHVR-Ig transfectant cells were prepared for SDS-polyacrylamide gel electrophoresis under reducing and nonreducing conditions in parallel with the indicated quantities of purified human (Hu) IgG1. After electrophoresis, proteins were transferred to nitrocellulose and incubated first with an ALP-conjugated antibody directed against human Ig and then with an ALP enzyme substrate solution. Localized deposition of the purple enzyme product is shown. MW_r, relative molecular weight (in thousands).

100-kDa dimer under reducing and nonreducing conditions, respectively. The signals indicating the synthesis and secretion of sMHVR-Ig were compared to those generated by known masses of human IgG1, whose heavy chains have a slightly slower mobility than that of sMHVR-Ig. A comparison of band intensities revealed that the amount of sMHVR-Ig in 1 μl of conditioned medium was between 0.01 and 0.1 μg (Fig. 1B).

Measurement of binding between the MHVR and MHV particles. Immobilization of sMHVR-Ig via its Fc domain would be expected to display the virus-binding $MHVR_{NTD}$ in a fashion analogous to that of authentic MHVR on cell surfaces, thereby permitting in vitro measurements of binding between purified virus and the receptor. Thus, the medium from 293 EBNA transfectants was mixed with Sepharose-protein G beads to noncovalently link the sMHVR-Ig to a solid phase. Initially, serial 0.5-log_{10} dilutions of the sMHVR-Ig medium were prepared with 293 EBNA growth medium as diluent, and then Sepharose-protein G beads were added to 0.1% (vol/vol). This was intended to generate a series of bead preparations of various receptor densities. Additionally, a parallel series of control beads containing the human Ig Fc domain but lacking the $MHVR_{NTD}$ were prepared by incubation with dilutions of sCD30-Ig (17, 41a). sCD30-Ig was produced by 293 EBNA cells stably transfected with the pCEP4:sCD30-Ig construct.

The recombinant Fc-containing proteins that bound to the beads present in 0.1-ml volumes were identified by immunoblotting (Fig. 2A). All preparations contained bovine IgG, whose heavy chain was evident as a broad ca. 50-kDa band. This bovine IgG, which was derived from the FCS present in growth medium, bound strongly to Sepharose-protein G. More importantly, the expected increases in sMHVR-Ig (ca. 45 kDa) and sCD30-Ig (ca. 100 kDa due to the 359-residue CD30 ectodomain) were evident and the anticipated masses of recombinant protein per 0.1-ml bead suspensions were confirmed by comparing immunoblot signal intensities with those generated by known masses of human IgG1 (Fig. 2A).

To measure the virus-receptor interaction, these two series of Sepharose bead preparations were incubated overnight at 4°C with gradient-purified ^{35}S-labelled MHV particles and the radioactivity adsorbed to pelleted beads was quantitated. The MHV strains chosen for these analyses were the prototype JHM (strain 4) and the tissue culture-adapted JHMX variant (43). These strains were selected primarily because JHMX is known to be a JHM derivative that lacks 153 residues within S1 (48, 59) and thus the role of this S1 deletion in receptor binding could be explored.

For both JHM and JHMX, the proportion of particles bound to beads after overnight incubation at 4°C increased with increasing density of immobilized sMHVR (Fig. 2B). Typically, JHM virion preparations contained a relatively low proportion of particles able to bind to sMHVR (maximum of 41% [Fig. 2]), while JHMX preparations exhibited significantly higher levels of binding. For both JHM and JHMX, increases in virion adsorption were not observed in conjunction with increasing densities of the control sCD30-Ig; indeed, the radioactivity associated with the entire Sepharose–CD30-Ig series was not significantly different from background levels of counts. Thus, the increases in virion adsorption with increasing sMHVR-Ig levels were specific to the sMHVR domain and did not result from binding to the human Ig Fc region, as might have been suggested by the reported affinity of the MHV S protein for Fc domains (47).

Strain-specific elution of virus from the MHVR at 37°C. In vitro interaction between virus and the receptor was stable at 4°C, but a shift to 37°C resulted in a remarkable strain-specific elution. This was discovered when Sepharose–sMHVR-Ig beads containing bound virions were shifted to 37°C for 1 h. The majority of the receptor-associated JHM eluted, while

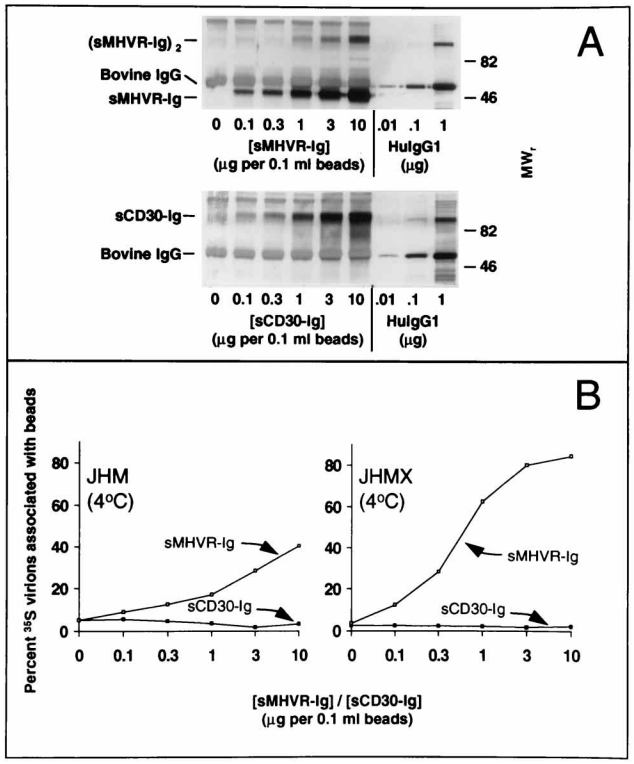

FIG. 2. Effect of sMHVR density on in vitro adsorption of ^{35}S-labelled MHV particles. Serial 0.5-$\log_{10}$ dilutions of media containing either sMHVR-Ig or sCD30-Ig were prepared with DMEM–10% ΔFCS as diluent and then incubated with Sepharose-protein G (0.1% [vol/vol]) until all recombinant proteins were quantitatively bound to beads. Beads were then rinsed extensively with PBS and resuspended to 1% (vol/vol) in DMEM–1% ΔFCS. (A) Aliquots (0.1 ml) of each 1% (vol/vol) suspension were removed, beads were pelleted, and the associated proteins were analyzed in parallel with the indicated human IgG1 (HuIgG1) standards by immunoblotting, as described in the legend to Fig. 1. MW_r, relative molecular size (in kilodaltons). (B) Aliquots (0.1 ml) of each 1% (vol/vol) suspension were mixed with purified ^{35}S-labelled virions (10^4 cpm) in 1 ml of DMEM–1% ΔFCS. After a 24-h incubation at 4°C, beads were pelleted and unbound virions were removed. Beads were rinsed once with cold DMEM–1% ΔFCS, repelleted, and suspended in 1 ml of 1% SDS to dissolve bound virions. The fraction of original ^{35}S present in the SDS solutions was determined and plotted as the proportion of bead-associated radioactivity.

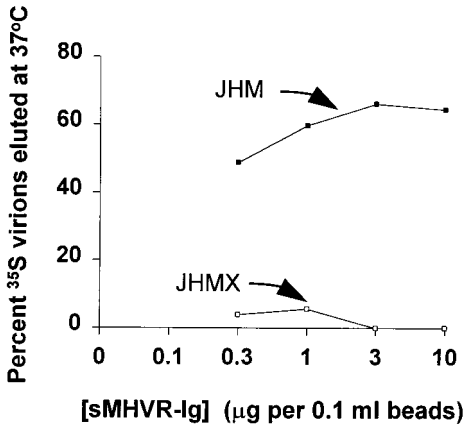

FIG. 3. Elution of JHM, but not JHMX, from Sepharose–sMHVR-Ig beads at 37°C. ^{35}S-labelled virions were bound at 4°C to Sepharose–sMHVR-Ig beads, unbound virions were removed, and beads were resuspended in DMEM—1% ΔFCS, all as described in the legend to Fig. 2. Samples were then incubated for 1 h at 37°C. Beads were pelleted, and the proportions of ^{35}S radioactivity eluted into supernatants due to 37°C exposure were determined by scintillation counting. Elution data for samples containing low receptor densities are not presented because the amounts of ^{35}S-labelled JHM released from suspensions containing less than 0.3 μg of sMHVR-Ig per 0.1 ml were too small to permit accurate quantitation.

JHMX remained with the Sepharose beads (Fig. 3). The specific failure of JHM to maintain a stable association with the receptor at a physiologic temperature and pH was evident throughout a 1.5-$\log_{10}$ range of receptor densities.

Radiolabelled virions that were bound to sMHVR-Ig at 4°C and then subsequently released at 37°C were collected and monitored for both radioactive content and infectivity (Fig. 4). In this experiment, high levels of ^{35}S-labelled virions (10^5 cpm/ml) were used; this allowed the measurement of virion elution from low-receptor-density beads. As expected, relatively low levels of JHMX-specific radioactivity eluted from receptor-containing beads at 37°C (Fig. 4). While some infectious virus was present in these eluates, none appeared to be specifically due to elution from the receptor, as titers in eluates above receptor-containing beads were actually lower than those found above beads lacking the receptor. A far more interesting elution pattern was observed when JHM was examined (Fig. 4). For JHM, infective ^{35}S-labelled virus was released from beads containing low receptor densities (0.1 to 1.0 μg of sMHVR-Ig per 0.1-ml beads); these eluates had titers higher than those of corresponding eluates from beads lacking sMHVR-Ig. However, the abundant amounts of ^{35}S-labelled JHM released from beads with the highest receptor densities clearly lacked infectivity.

Initial attempts to identify biochemical distinctions between infectious JHM and noninfectious JHM released from high-density sMHVR beads involved the electrophoretic comparison of their ^{35}S-labelled virion proteins (Fig. 5). In these electrophoretic profiles, the critical receptor-binding S proteins of JHM were evident as a thin ca. 100-kDa band of S1 and a more-diffuse ca. 90-kDa band of S2 (Fig. 5, lanes 1 through 5). Despite the incomplete separation of these S1 and S2 proteins, the profiles did show similar levels of S, nucleocapsid, and matrix proteins among input JHM virions (Fig. 5, lane 1) and virions bound to the receptor at 4°C (lane 3). More importantly, the side-by-side comparison of virion proteins that remained on receptor beads after 37°C exposure (Fig. 5, lane 5) with those that eluted (lane 4) showed that the peripheral S1 ligand was primarily associated with the receptor beads, while the majority of the integral membrane S2 fragment was in the eluted material. Together, these findings suggested that at least some of the JHM released from high-density sMHVR beads involved dissociation at the S1-S2 junction.

The S1 polypeptide of JHMX is 20% smaller than that of JHM; therefore, JHMX S1 and S2 chains coelectrophorese (Fig. 5, lanes 6 through 10). Despite this situation, the electrophoretic profiles of the JHMX proteins verified that the vast majority of virions were not released from beads at 37°C (Fig. 5, lanes 9 and 10). These results were consistent with a more stable association of JHMX S1 and S2 chains.

Strain-specific elution of virus from tissue culture cells producing the MHVR. The detection of infectious JHM release from Sepharose beads containing a low density of immobilized sMHVR-Ig indicated that a similar release process might occur on the surface of a receptor-positive cell. This possibility was investigated by allowing ^{35}S-labelled virions to bind overnight at 4°C to HeLa cells stably transfected with the complete MHVR gene (30). After this binding, HeLa-MHVR cells were rinsed extensively and the kinetics of virion elution into culture

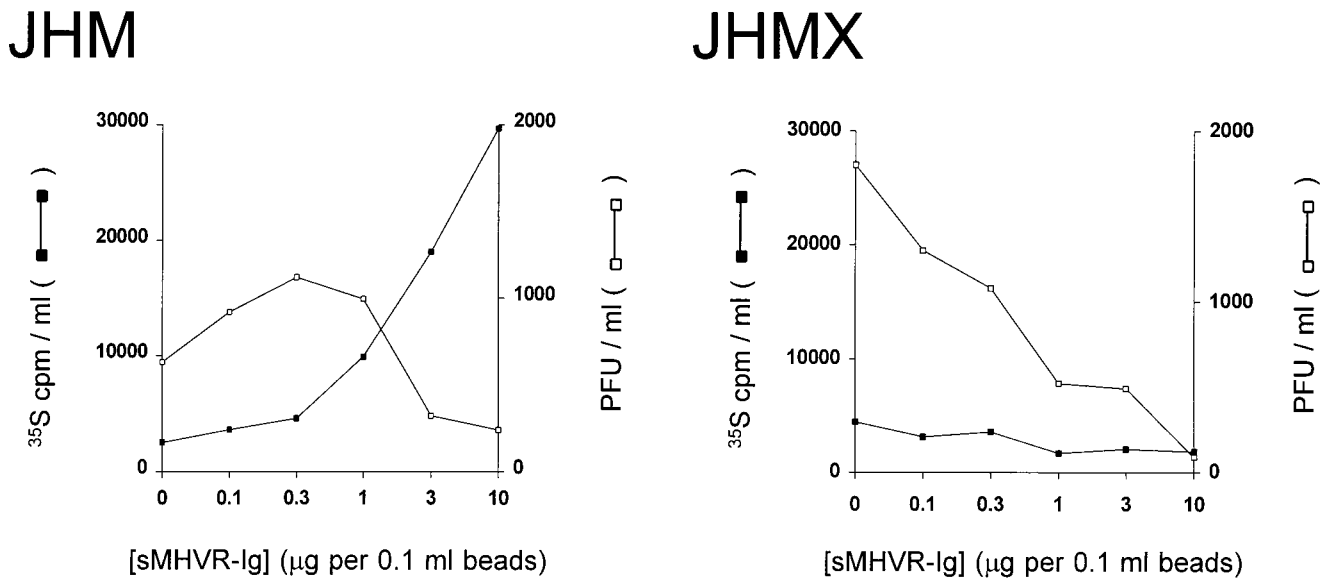

FIG. 4. Infectivity of MHV particles eluted from Sepharose–sMHVR-Ig beads at 37°C. Input ^{35}S-labelled MHV particles (10^5 cpm/ml) (JHM, 9 PFU/cpm; JHMX, 16 PFU/cpm) were bound to Sepharose–sMHVR-Ig beads at 4°C, as described in the legend to Fig. 2, and subsequently eluted from beads at 37°C, as described in the legend to Fig. 3. The radioactivities present in eluates were determined by scintillation counting. The infectivities of eluted virions were determined by plaque assays with HeLa-MHVR indicator cell monolayers.

media was determined by scintillation spectrometry and plaque assays.

The HeLa-MHVR cells employed in these experiments (clone 3) reproducibly bound a relatively small proportion of input virions, 19% ± 3.4% for JHM and 31.5% ± 1.3% for JHMX ($x \pm \sigma n$; $n = 3$). As expected, these cell-associated ^{35}S-labelled virions did not elute into media when the temperature was held at 4°C (Fig. 6A). However, parallel 37°C incubations caused the rapid release of 10 to 12% of JHM particles. In contrast, a much more limited elution of only 1 to 2% of JHMX particles was observed (Fig. 6A). Thus, these results correlated well with those obtained from in vitro binding assays.

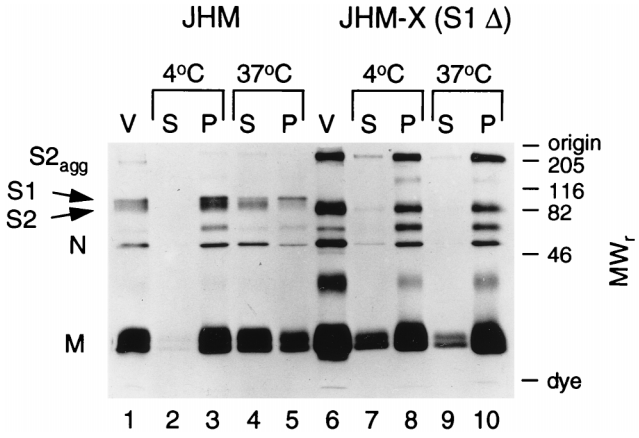

FIG. 5. Electrophoretic profiles of virion proteins before and after virion association with high-density Sepharose-sMHVR beads. ^{35}S-labelled virions (3.4×10^4 cpm) were allowed to bind to the receptor by incubation at 4°C for 18 h in 1 ml of DMEM–10% ΔFCS containing 10 μg of sMHVR-Ig and 0.1% (vol/vol) Sepharose-protein G. Sepharose beads were then pelleted by centrifugation and washed twice with 1 ml of ice-cold DMEM–0.1% ΔFCS. A 10% suspension was prepared, and aliquots were either held at 4°C or incubated for 1 h at 37°C. Sepharose beads were pelleted, and radioactive proteins associated with the supernatants (S lanes) and pellets (P lanes) were separated by reducing SDS-polyacrylamide gel electrophoresis and visualized by fluorography. V lanes depict the electrophoretic profiles of ^{35}S-labelled virion proteins prior to incubation. The positions of molecular size standards (in kilodaltons) are indicated on the right. M, membrane; N, nucleocapsid; $S2_{agg}$, S2 aggregate.

The capacity of cells to adsorb ^{35}S-labelled virions (19% for JHM) was roughly equivalent to that of Sepharose beads containing intermediate (0.3 to 1.0 μg per 0.1 ml) sMHVR densities (Fig. 2). Since the JHM virions released from beads with these receptor densities were found to be infective in plaque assays (Fig. 4), the elution of infective JHM from cells was anticipated. This was indeed observed. Infective JHM, but not JHMX, eluted specifically in response to 37°C exposure (Fig. 6B). JHM was found in culture media after 10 min at 37°C at 860 PFU/ml (Fig. 6B) and 405 cpm/ml (Fig. 6A). Thus, the specific infectivity of this eluted virus (2.1 PFU/cpm) was similar to the original input JHM (3.1 PFU/cpm); binding to cells and subsequent elution had little effect on virion infectivity. Prolonged (20- to 30-min) exposures at 37°C decreased JHM-specific infectivity (Fig. 6). This was not surprising; thermolability is a well-described characteristic of the JHM strain.

JHM S proteins lacking S1 residues 446 to 598 maintain a stable association with sMHVR-Ig, while complete JHM S proteins do not. To determine whether the 153-residue S1 deletion of JHMX is in fact the alteration responsible for the maintenance of receptor association, sMHVR-Ig was adsorbed to cells bearing a complete S protein or to parallel cell cultures bearing S proteins lacking residues 446 to 598 (designated $S_{\Delta S1}$). To obtain S-expressing cells, vaccinia virus vectors capable of producing the two types of S protein were prepared as described in Materials and Methods. HeLa cells were then coinfected with vTF7.3 (26) and the respective vTM1-S or vTM1-$S_{\Delta S1}$ vaccinia virus recombinant. S proteins were produced, as judged by syncytium-forming capacity and electrophoretic analysis of ^{35}S-labelled intracellular proteins. Both the complete S protein and $S_{\Delta S1}$ were powerfully syncytiogenic in HeLa-MHVR cells, and the $S_{\Delta S1}$ product had the relatively

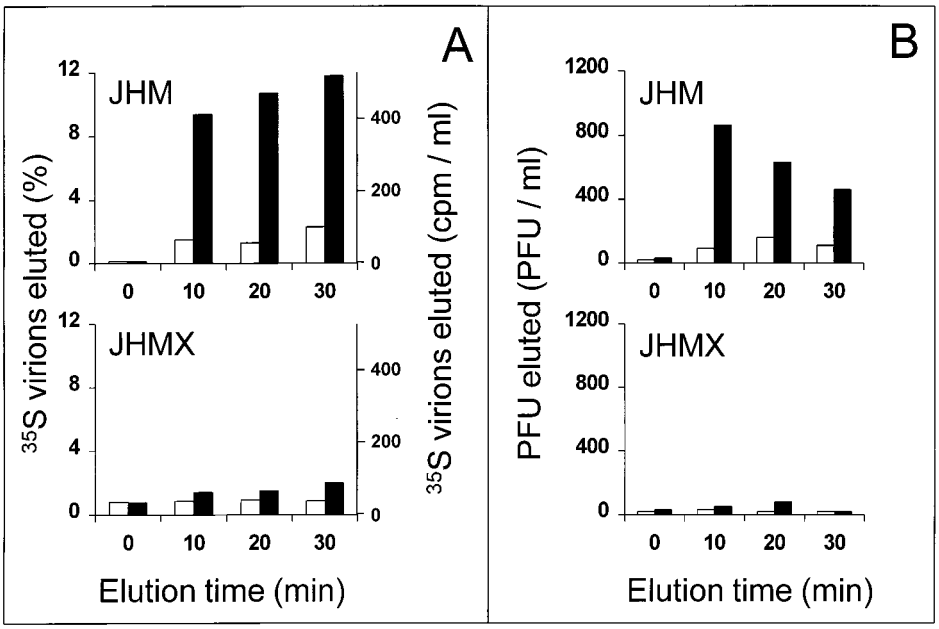

FIG. 6. Elution of JHM, but not JHMX, from HeLa-MHVR cells at 37°C. Purified ^{35}S-labelled virions (JHM, 3.1 PFU/cpm; JHMX, 6.5 PFU/cpm) were diluted in DMEM–0.1% ΔFCS to 2×10^5 PFU/ml. Then 0.5-ml aliquots were added to 10^6 HeLa-MHVR cells and left for 14 h at 4°C. Unadsorbed virions were removed, cells were rinsed extensively, and then ice-cold DMEM–0.1% ΔFCS (0.5 ml per 10^6 cells) was added. After the indicated elution periods, the medium was removed and cell monolayers were dissolved in DMEM–0.1% ΔFCS containing 1% NP-40 (0.5 ml per 10^6 cells). (A) After the radioactivities associated with media and cell lysates were determined, the percentages of ^{35}S present in media, as well as the counts of ^{35}S per minute per milliliter of medium, were plotted as a function of elution time. (B) The infectivities associated with media were determined by plaque assays with HeLa-MHVR indicator cells. □, 4°C elution; ■, 37°C elution.

rapid electrophoretic mobility expected for a large S1 deletion (data not shown). Thus, cultures in which cells displayed S proteins that differed only in the presence or absence of S1 residues 446 to 598 were established.

At 4°C, sMHVR-Ig bound specifically to HeLa cells bearing either S or $S_{\Delta S1}$ (Fig. 7). sMHVR-Ig interaction with $S_{\Delta S1}$ differed from the parallel interaction with complete S proteins in two ways. First, cells displaying $S_{\Delta S1}$ retained a relatively high proportion of sMHVR-Ig (Fig. 7). This was expected, as JHMX virions were superior to JHM virions in adsorption to sMHVR-Ig (Fig. 2). Second, cells bearing $S_{\Delta S1}$ retained the majority of sMHVR-Ig throughout a 1-h incubation at 37°C (Fig. 7). This finding contrasted with the rapid and abundant elution of sMHVR-Ig from cells bearing the complete S protein, where over 50% of sMHVR-Ig was released from cells after only 15 min at 37°C (Fig. 7). Thus, the deletion mutation examined here was capable of significantly enhancing the S protein's ability to maintain association with the MHVR at 37°C.

DISCUSSION

To examine the effects of MHV S protein mutations on receptor interaction, assays in which MHV could bind to its receptor under defined in vitro conditions were developed. Two different isolates of MHV were assayed, and a relationship between a deletion mutation and stable receptor association was revealed. This finding has implications for the evolution and pathogenesis of MHV infections.

MHV deletion mutants may be selectively amplified because they maintain association with cellular receptors. Viral RNA-dependent RNA replication results in spontaneous mutants that often exhibit selective advantages over the parent virus and therefore predominate after long-term growth. This is exemplified in a remarkable way during MHV (strain JHM) infections, where viable deletion mutations eliminating about 10% of S protein-encoding sequences are observed (3, 48). Such a deletion event is thought to occur during elongation of genomic RNA when the RNA-dependent polymerase makes a rare template switch (35, 39). In tissue culture, the resulting

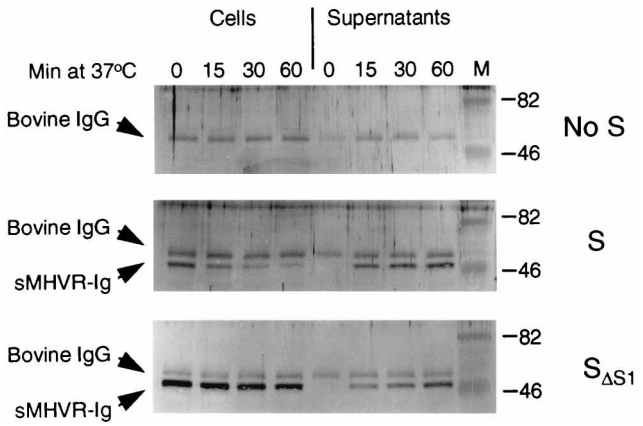

FIG. 7. Effect of a deletion in S1 on the capacity of S proteins to maintain association with sMHVR-Ig. HeLa cells (10^6 per well) were infected with vaccinia virus recombinants lacking the S gene (no S) or encoding the complete MHV4 S protein (S) or the mutant form of MHV4 S protein in which S1 residues 446 to 598 are absent ($S_{\Delta S1}$). Twelve hours later, cells were chilled on ice and overlaid with ice-cold sMHVR-Ig (10 μg per well in 1 ml of DMEM–10% ΔFCS). After 2 h at 4°C, unbound sMHVR-Ig was removed and replaced with ice-cold DMEM–0.1% ΔFCS containing 5 μg of brefeldin A per ml (1 ml per well). At the indicated times after a shift to 37°C, supernatants were removed and cell sheets were dissolved in DMEM–0.1% ΔFCS containing 0.5% NP-40 (1 ml per well). sMHVR-Ig in cell and supernatant fractions was precipitated with Sepharose-protein G and identified by Western immunoblotting as described in Materials and Methods. The amount of sample loaded per lane corresponds to the protein G-bound material from 0.5 ml of cell lysate or supernatant. IgG heavy chains due to a cross-reaction between the immunoblot detection reagent and FCS-derived bovine IgG appeared; these bands served as a sample loading control. Lane M, molecular size markers (in kilodaltons).

mutants typically grow to titers 10 to 100 times that of the parent JHM, which has a complete S protein (28, 49).

Multiple factors likely drive positive selection of S1 deletion variants. At least in some tissue culture lines, deletion variants are less cytocidal than is the parent JHM (28), thereby allowing for prolonged support of variant progeny. This report provides an additional fundamental explanation for the selection of deletion mutants. The variant tested here is superior to its parent in maintaining association with the MHVR. This increases the likelihood of productive cell entry by the variant.

This finding is consistent with elegant studies of DBT and 17 cl 1 cells persistently infected with MHV (strain A59). In these cultures, a selective process occurs during viral persistence that results in relatively virus-resistant cells containing dramatically reduced levels of the MHVR (52). Coevolution of virus also occurs, giving rise to variants able to maintain the ability to infect cells with the low-density MHVR (11). One might speculate that the variants within these persistently infected cultures contain numerous different S mutations, each of which enhances the stability of MHV association with the receptor. Indeed, that mutations other than S1 deletions might be important in this process is suggested by the results in Fig. 7. S proteins lacking S1 residues 446 to 598 interact more stably with the receptor than do complete S proteins, but even with this deletion, S proteins fail to quantitatively retain the receptor at 37°C. Presently unrecognized additional changes in S proteins that further contribute to the stable binding phenotype might include point mutations in the S protein which alter membrane fusion function (6, 29, 31) or overall S conformation (33).

Maintenance of virus-receptor interaction may be enhanced by a stable association between virion proteins S1 and S2. S1 residues bind to the MHVR (58), yet S1 fragments are known to be noncovalently associated with S2 and can in fact detach from virions under relatively mild conditions of slightly alkaline pH (8, 57). These findings suggest that some MHV particles which have bound the receptor via the S1 ligand quickly elute, leaving S1 bound to the receptor. The results presented here support this contention, as the JHM eluted from Sepharose-sMHVR beads was depleted of S1 (Fig. 5). In this study, convincing S1 depletion was identified among the noninfectious particles dissociated from high-density sMHVR beads. Conceivably, the extent of the S1 loss from these viruses leaves them with too little ligand to bind and infect the HeLa-MHVR cells used to monitor infectivity. Retention of S1 on low-density Sepharose-sMHVR beads and HeLa-MHVR cells is liable to be far less extensive, and therefore, infective virus can be observed in 37°C eluates (Fig. 4 and 6).

The restricted tropism of the JHM strain may be due to its inability to maintain association with the MHVR. The genes encoding receptors other than the primary MHVR have been identified by cDNA transfection of MHV-resistant, receptor-negative cell lines. cDNAs able to express a product which confers susceptibility to MHV infection are designated MHVR genes (10, 19, 46, 67, 68). Interestingly, these alternative MHVR transfectants often show a peculiar resistance to the MHV JHM strain. For example, a recently discovered brain-specific receptor (brain CEA) renders Cos7 cells susceptible to infection by MHV strains A59, 2, and 3, but not the JHM strain (10). Additionally, an allelic isoform of the primary MHVR, when present on the surface of murine SJL cells, confers sensitivity to infection by MHV strain A59, but not JHM (67). These findings have prompted suggestions that accessory factors other than the surface receptor are required specifically for JHM entry or that an additional as-yet-unidentified JHM-specific receptor(s) must exist (2). Additional receptors are indeed likely to be found as known receptors to date are members of a very large gene family (44). However, resistance to JHM in transfectant and SJL cells might be due in large part to an unstable association between JHM and the receptor. This view is supported by the results of Pasick et al. (49), who found that SJL-derived glial cells were resistant to infection by JHM virus but were sensitive to infection by variants of JHM possessing deletions within S1. In preliminary comparative studies, MHV strain A59 has been found to exhibit extraordinarily high levels of thermostable binding to the MHVR (49a). Therefore, the likelihood of JHM elution from the cell surface, particularly from a cell surface with a low-affinity, alternative MHVR and/or low MHVR density, is higher than that of A59. This might render many cells unable to permit the successful penetration of the JHM strain in a 1-h 37°C incubation.

The kinetics of JHM dissemination in vivo may relate to the propensity of virus to elute from cell surface receptors. It is in the in vivo environment of the murine central nervous system (CNS) that JHM propagates more rapidly than does its deletion mutant offspring. JHM was in fact isolated after serial inoculations of infective brain homogenates through suckling mouse brain (63). After in vivo infection, in situ localization of MHV4 (JHM) RNA indicates a largely transneuronal spread through the CNS that is extremely rapid, regardless of whether the virus is administered intracerebrally (14) or intranasally (4). Relative to MHV4 (JHM), all other known MHV strains are neuroattenuated. Several studies have shown that attenuated MHV strains spread and infect the same neuroanatomic structures as does JHM but that they do so more slowly and with less dissemination of infection (23, 41). How might these kinetic differences be explained? One possibility is that rapid MHV4 elution from cell surfaces provides it with the ability to disseminate widely and rapidly in the CNS from individual sites of single-cell infection. On the other hand, MHV4 variants, many of which harbor deletions within S1, may remain localized to discrete foci due to the maintenance of receptor association.

ACKNOWLEDGMENTS

Superb technical support was provided by Sean Kelly. Additional thanks go to Kathy Cho for assistance in preparing recombinant vaccinia virus vectors. I thank Hans Martin Jäck for providing the pCEP4: sCD30 vector and for essential advice on construction of pCEP4: sMHVR-Ig. I also thank Griffith Parks and Stanley Perlman for critical reading of the manuscript.

This research was supported by NIH grant NS31636 and by a grant from the Schweppe Foundation of Chicago.

REFERENCES

1. **Adami, C., J. Pooley, J. Glomb, E. Stecker, F. Fazal, J. O. Fleming, and S. C. Baker.** 1995. Evolution of MHV during chronic infection: quasispecies nature of the persisting MHV RNA. Virology **209:**337–346.
2. **Asanaka, M., and M. M. C. Lai.** 1993. Cell fusion studies identified multiple cellular factors involved in mouse hepatitis virus entry. Virology **197:**732–741.
3. **Banner, L. R., J. G. Keck, and M. M. Lai.** 1990. A clustering of RNA recombination sites adjacent to a hypervariable region of the peplomer gene of murine coronavirus. Virology **175:**548–555.
4. **Barnett, E., M. Cassell, and S. Perlman.** 1993. Two neurotropic viruses, herpes simplex virus type 1 and mouse hepatitis virus, spread along different neural pathways from the main olfactory bulb. Neuroscience **157:**1007–1025.
5. **Bates, P. A., J. Luo, and M. J. E. Sternberg.** 1992. A predicted three-dimensional structure for the carcinoembryonic antigen (CEA). FEBS Lett. **301:**207–214.
6. **Bos, E. C. W., L. Heijnen, W. Luytjes, and W. J. M. Spaan.** 1995. Mutational analysis of the murine coronavirus spike protein: effect on cell-to-cell fusion. Virology **214:**453–463.
7. **Castro, R., and S. Perlman.** 1995. $CD8^+$ T-cell epitopes within the surface glycoprotein of a neurotropic coronavirus and correlation with pathogenicity. J. Virol. **69:**8127–8131.

8. **Cavanagh, D.** 1995. The coronavirus surface glycoprotein, p. 73–113. *In* S. G. Siddell (ed.), The coronaviridae. Plenum Press, New York, N.Y.
9. **Cavanagh, D., P. J. Davis, and A. P. Mockett.** 1988. Amino acids within hypervariable region 1 of avian coronavirus IBV (Massachusetts serotype) spike glycoprotein are associated with neutralization epitopes. Virus Res. **11:**141–150.
10. **Chen, D. S., M. Asanaka, K. Yokomori, F. Wang, S. B. Hwang, H. Li, and M. M. C. Lai.** 1995. A pregnancy-specific glycoprotein is expressed in the brain and serves as a receptor for mouse hepatitis virus. Proc. Natl. Acad. Sci. USA **92:**12095–12099.
11. **Chen, W., and R. S. Baric.** 1996. Molecular anatomy of mouse hepatitis virus persistence: coevolution of increased host cell resistance and virus virulence. J. Virol. **70:**3947–3960.
12. **Chomczynski, P., and N. Sacchi.** 1987. Single-step method of RNA isolation by acid guanidinium thiocyanate-phenol-chloroform extraction. Anal. Biochem. **162:**156–159.
13. **Collins, A. R., R. L. Knobler, H. Powell, and M. J. Buchmeier.** 1982. Monoclonal antibodies to murine hepatitis virus-4 (strain JHM) define the viral glycoprotein responsible for attachment and cell-cell fusion. Virology **119:** 358–371.
14. **Dalziel, R. G., P. W. Lampert, P. J. Talbot, and M. J. Buchmeier.** 1986. Site-specific alteration of murine hepatitis virus type 4 peplomer glycoprotein E2 results in reduced neurovirulence. J. Virol. **59:**463–471.
15. **Davies, H. A., and M. R. Macnaughton.** 1979. Comparison of the morphology of three coronaviruses. Arch. Virol. **59:**25.
16. **Delmas, B., and H. Laude.** 1990. Assembly of coronavirus spike protein into trimers and its role in epitope expression. J. Virol. **64:**5367–5375.
17. **Dürkop, H., U. Latza, M. Hummel, F. Eitelbach, B. Seed, and H. Stein.** 1992. Molecular cloning and expression of a new member of the nerve growth factor receptor family that is characteristic for Hodgkin's disease. Cell **68:** 421–427.
18. **Dveksler, G. S., M. N. Pensiero, C. B. Cardellichio, R. K. Williams, G.-S. Jiang, K. V. Holmes, and C. W. Dieffenbach.** 1991. Cloning of the mouse hepatitis virus (MHV) receptor: expression in human and hamster cell lines confers susceptibility to MHV. J. Virol. **65:**6881–6891.
19. **Dveksler, G. S., C. W. Dieffenbach, C. B. Cardellichio, K. McCuaig, M. N. Pensiero, G.-S. Jiang, N. Beauchemin, and K. V. Holmes.** 1993. Several members of the mouse carcinoembryonic antigen-related glycoprotein family are functional receptors for the coronavirus mouse hepatitis virus-A59. J. Virol. **67:**1–8.
20. **Dveksler, G. S., M. N. Pensiero, C. W. Dieffenbach, C. B. Cardellichio, A. A. Basile, P. E. Elia, and K. V. Holmes.** 1993. Mouse coronavirus MHV-A59 and blocking anti-receptor monoclonal antibody bind to the N-terminal domain of cellular receptor MHVR. Proc. Natl. Acad. Sci. USA **90:**1716–1720.
21. **Dveksler, G. S., S. E. Gagneten, C. A. Scanga, C. B. Cardellichio, and K. V. Holmes.** 1996. Expression of the recombinant anchorless N-terminal domain of mouse hepatitis virus (MHV) receptor makes hamster or human cells susceptible to MHV infection. J. Virol. **70:**4142–4145.
22. **Ellison, J. W., B. J. Berson, and L. E. Hood.** 1982. The nucleotide sequence of a human immunoglobulin C-gamma-1 gene. Nucleic Acids Res. **10:**4071–4079.
23. **Fazakerley, J. K., S. Parker, F. Bloom, and M. J. Buchmeier.** 1992. The V5A13.1 envelope glycoprotein deletion mutant of mouse hepatitis virus type-4 is neuroattenuated by its reduced rate of spread in the central nervous system. Virology **187:**178–188.
24. **Felgner, P. L., T. R. Gadek, M. Holm, R. Roman, H. W. Chan, M. Wenz, J. P. Northrop, G. M. Ringold, and M. Danielsen.** 1987. Lipofection: a highly efficient, lipid-mediated DNA-transfection procedure. Proc. Natl. Acad. Sci. USA **84:**7413–7417.
25. **Frana, M. F., J. N. Behnke, L. S. Sturman, and K. V. Holmes.** 1985. Proteolytic cleavage of the E2 glycoprotein of murine coronavirus: host-dependent differences in proteolytic cleavage and cell fusion. J. Virol. **56:**912–920.
26. **Fuerst, T. R., P. L. Earl, and B. Moss.** 1987. Use of a hybrid vaccinia virus-T7 RNA polymerase system for expression of target genes. Mol. Cell. Biol. **7:**2538–2544.
27. **Gagneten, S., O. Gout, M. Dubois-Dalcq, P. Rottier, J. Rossen, and K. V. Holmes.** 1995. Interaction of mouse hepatitis virus (MHV) spike glycoprotein with receptor glycoprotein MHVR is required for infection with an MHV strain that expresses the hemagglutinin-esterase glycoprotein. J. Virol. **69:**889–895.
28. **Gallagher, T. M., S. E. Parker, and M. J. Buchmeier.** 1990. Neutralization-resistant variants of a neurotropic coronavirus are generated by deletions within the amino-terminal half of the spike glycoprotein. J. Virol. **64:**731–741.
29. **Gallagher, T. M., C. Escarmis, and M. J. Buchmeier.** 1991. Alteration of the pH dependence of coronavirus-induced cell fusion: effect of mutations in the spike glycoprotein. J. Virol. **65:**1916–1928.
30. **Gallagher, T. M.** 1996. Murine coronavirus membrane fusion is blocked by modification of thiols buried within the spike protein. J. Virol. **70:**4683–4690.
31. **Gombold, J. L., S. T. Hingley and S. R. Weiss.** 1993. Fusion-defective mutants of mouse hepatitis virus A59 contain a mutation in the spike protein cleavage signal. J. Virol. **67:**4504–4512.
32. **Gossen, M., and H. Bujard.** 1992. Tight control of gene expression in mammalian cells by tetracycline-responsive promoters. Proc. Natl. Acad. Sci. USA **89:**5547–5551.
33. **Grosse, B., and S. G. Siddell.** 1994. Single amino acid changes in the S2 subunit of the MHV surface glycoprotein confer resistance to neutralization by S1 subunit-specific monoclonal antibody. Virology **202:**814–824.
34. **Holmes, K. V., and G. S. Dveksler.** 1994. Specificity of coronavirus/receptor interactions, p. 403–443. *In* E. Wimmer (ed.), Cellular receptors for animal viruses. Cold Spring Harbor Laboratory Press, Cold Spring Harbor, N.Y.
35. **Huang, A. S., and D. Baltimore.** 1977. Defective interfering animal viruses, p. 73–116. *In* H. Frankel-Conrat and R. R. Wagner (ed.), Comprehensive virology. Plenum Press, New York, N.Y.
36. **Innis, M. A., and D. H. Gelfand.** 1990. Optimization of PCRs, p. 3–12. *In* M. A. Innis, D. H. Gelfand, J. J. Sninsky, and T. J. White (ed.), PCR protocols. Academic Press, Inc., San Diego, Calif.
37. **Kawasaki, E. S.** 1990. Amplification of RNA, p. 21–27. *In* M. A. Innis, D. H. Gelfand, J. J. Sninsky, and T. J. White (ed.), PCR protocols. Academic Press, Inc., San Diego, Calif.
38. **Krijnse Locker, J., M. Ericsson, P. J. M. Rottier, and G. Griffiths.** 1994. Characterization of the budding compartment of mouse hepatitis virus: evidence that transport from the RER to the Golgi complex requires only one vesicular transport step. J. Cell Biol. **124:**55–70.
39. **Lai, M. M.** 1992. Genetic recombination in RNA viruses. Curr. Top. Microbiol. Immunol. **176:**21–32.
40. **Laude, H., K. Van Reeth, and M. Pensaert.** 1993. Porcine respiratory coronavirus: molecular features and virus-host interactions. Vet. Res. **24:**125–150.
41. **Lavi, E., P. S. Fishman, M. K. Highkin, and S. R. Weiss.** 1988. Limbic encephalitis after inhalation of a murine coronavirus. Lab. Invest. **58:**31–36.

41a. **Li, T., and H. M. Jäck.** Unpublished data.

42. **Mackett, M., G. L. Smith, and B. Moss.** 1984. General method for production and selection of infectious vaccinia virus recombinants expressing foreign genes. J. Virol. **49:**857–864.
43. **Makino, S., F. Taguchi, M. Hayami, and K. Fujiwara.** 1983. Characterization of small plaque mutants of mouse hepatitis virus, JHM strain. Microbiol. Immunol. **27:**445–454.
44. **McCuaig, K., M. Rosenberg, P. Nedellec, C. Turbide, and N. Beauchemin.** 1993. Expression of the Bgp gene and characterization of mouse colon biliary glycoprotein isoforms. Gene **127:**173–183.
45. **Moss, B., O. Elroy-Stein, T. Mizukami, W. A. Alexander, and T. R. Fuerst.** 1990. New mammalian expression vectors. Nature **348:**91–92.
46. **Nedellec, P., G. S. Dveksler, E. Daniels, C. Turbide, B. Chow, A. A. Basile, K. V. Holmes, and N. Beauchemin.** 1994. *Bgp2*, a new member of the carcinoembryonic antigen-related gene family, encodes an alternative receptor for mouse hepatitis viruses. J. Virol. **68:**4525–4537.
47. **Oleszak, E. L., S. Perlman, and J. L. Leibowitz.** 1992. MHV S peplomer protein expressed by a recombinant vaccinia virus vector exhibits IgG Fc-receptor activity. Virology **186:**122–132.
48. **Parker, S. E., T. M. Gallagher, and M. J. Buchmeier.** 1989. Sequence analysis reveals extensive polymorphism and evidence of deletions within the E2 glycoprotein of several strains of murine hepatitis virus. Virology **173:**664–673.
49. **Pasick, J. M., G. A. Wilson, V. L. Morris, and S. Dales.** 1992. SJL/J resistance to mouse hepatitis virus-JHM-induced neurologic disease can be partially overcome by viral variants of S and host immunosuppression. Microb. Pathog. **13:**1–15.

49a. **Rao, P. V., and T. M. Gallagher.** Unpublished data.

50. **Sambrook, J., E. F. Fritsch, and T. Maniatis.** 1989. Molecular cloning: a laboratory manual, 2nd ed. Cold Spring Harbor Laboratory, Cold Spring Harbor, N.Y.
51. **Sanger, F., S. Nicklen, and A. R. Coulson.** 1977. DNA sequencing with chain-terminating inhibitors. Proc. Natl. Acad. Sci. USA **74:**5463–5467.
52. **Sawicki, S. G., J.-H. Lu, and K. V. Holmes.** 1995. Persistent infection of cultured cells with mouse hepatitis virus (MHV) results from the epigenetic expression of the MHV receptor. J. Virol. **69:**5535–5543.
53. **Siddell, S. G.** 1995. The small membrane protein, p. 181–189. *In* S. G. Siddell (ed.), The coronaviridae. Plenum Press, New York, N.Y.
54. **Spaan, W., D. Cavanagh, and M. C. Horzinek.** 1988. Coronaviruses: structure and genome expression. J. Gen. Virol. **69:**2939–2952.
55. **Sturman, L. S., and K. K. Takemoto.** 1972. Enhanced growth of a murine coronavirus in transformed mouse cells. Infect. Immun. **6:**501–507.
56. **Sturman, L. S., C. S. Ricard, and K. V. Holmes.** 1985. Proteolytic cleavage of the E2 glycoprotein of murine coronavirus: activation of cell-fusing activity of virions by trypsin and separation of two different 90K cleavage fragments. J. Virol. **56:**904–911.
57. **Sturman, L. S., C. S. Ricard, and K. V. Holmes.** 1990. Conformational change of the coronavirus peplomer glycoprotein at pH 8.0 and 37°C correlates with virus aggregation and virus-induced cell fusion. J. Virol. **64:**3042–3050.
58. **Suzuki, H., and F. Taguchi.** 1996. Analysis of the receptor-binding site of murine coronavirus spike protein. J. Virol. **70:**2632–2636.

59. **Taguchi, F., and J. O. Fleming.** 1989. Comparison of six different murine coronavirus JHM variants by monoclonal antibodies against the E2 glycoprotein. Virology **169:**233–235.
60. **Taguchi, F.** 1995. The S2 subunit of the murine coronavirus spike protein is not involved in receptor binding. J. Virol. **69:**7260–7263.
61. **Tooze, J., S. A. Tooze, and G. Warren.** 1984. Replication of coronavirus MHV-A59 in sac− cells: determination of the first site of budding of progeny virions. Eur. J. Cell Biol. **33:**281–293.
62. **Vennema, H., L. Heignen, A. Zijderveld, M. C. Horzinek, and W. J. M. Spaan.** 1990. Intracellular transport of recombinant coronavirus spike proteins: implications for virus assembly. J. Virol. **64:**339–346.
63. **Weiner, L. P.** 1973. Pathogenesis of demyelination induced by a mouse hepatitis virus (JHM virus). Arch. Neurol. **28:**298–303.
64. **Wesley, R. D., R. D. Woods, and A. K. Cheung.** 1991. Genetic analysis of porcine respiratory coronavirus, an attenuated variant of transmissible gastroenteritis virus. J. Virol. **65:**3369–3373.
65. **Williams, R. K., G. S. Jiang, and K. V. Holmes.** 1991. Receptor for mouse hepatitis virus is a member of the carcinoembryonic antigen family of glycoproteins. Proc. Natl. Acad. Sci. USA **88:**5533–5536.
66. **Williams, R. K., G.-S. Jiang, S. W. Snyder, M. F. Frana, and K. V. Holmes.** 1990. Purification of the 110-kilodalton glycoprotein receptor for mouse hepatitis virus (MHV)-A59 from mouse liver and identification of a nonfunctional, homologous protein in MHV-resistant SJL/J mice. J. Virol. **64:**3817–3823.
67. **Yokomori, K., and M. M. C. Lai.** 1992. Mouse hepatitis virus utilizes two carcinoembryonic antigens as alternative receptors. J. Virol. **66:**6194–6199.
68. **Yokomori, K., and M. M. C. Lai.** 1992. The receptor for mouse hepatitis virus in the resistant mouse strain SJL is functional: implications for the requirement of a second factor for viral infection. J. Virol. **66:**6931–6938.